ISBN: 978-3-95450-248-6 ISSN: 2673-5490 doi: 10.18429/JACoW-IPAC2025-MOPB033

A NOVEL DESIGN OF A MAGNETIC CHICANE WITH POSITIVE R_{56}

H. Tanaka†, K. Soutome[1], T. Hara, RIKEN SPring-8 Center, Hyogo, Japan, City, Japan
[1]also at JASRI, Hyogo, Japan

Abstract

It has been attracting attention that the energy chirp, which is formed by the space-charge effect of the electron beam and the beam wake field when the beam passes through the accelerator tube, can be used to generate short-pulse XFELs. Since the energy chirp produced by this phenomenon is such that the energy of electrons in the rear of the bunch is lower than at the front, compression requires a magnetic chicane with a positive R_{56}, which shortens the path of the lower energy electrons. On the other hand, a normal simple electromagnetic chicane would have a negative R_{56}, not applicable to this bunch compression. In this presentation, we report on the idea of a compact R_{56}-positive magnetic chicane that can be inserted in a straight section, crucial considerations, and the tentative results of its design study.

INTRODUCTION

Recently, intense-attosecond XFEL generation was proven at European XFEL [1] by using a self-modulated energy chirp driven by space charge. This opens up the way to generate shorter pulsed XFEL at SACLA [2] beyond the current limitation on a pulse-duration of several femtosecond in FWHM. SACLA is the world first compact XFEL enabling efficient XFEL generation using low emittance single crystal 500-keV pulsed electron gun [3], C-band high-gradient RF accelerator [4] and short-period in-vacuum undulator [5] technologies. A high peak current beyond 10 kA [6] has been used routinely at SACLA to provide XFEL using relatively lower electron beam energy. Although this high-peak current operation has a merit to constantly provide a short pulsed XFEL of several femtosecond, large energy chirp over the bunch enhanced by a high peak current and high accelerator tube impedance is a de-merit by widening the XFEL spectrum significantly. If the troublesome energy chirp can be used to generate attosecond XFEL, namely, a pulse duration shorter than a femtosecond in FWHM, attosecond XFEL may has the potential to exploit a new scientific application at SACLA. From the above motivation, we started the design of a compact chicane with positive R_{56} for attosecond XFEL generation, which will be installed at BL3, the central XFEL beamline of SACLA.

SYSTEM MODIFICATION TOWARD ATTOSECOND XFEL GENERATION

SACLA can accommodate five FEL beamlines at maximum in the undulator hall. Currently three FEL beamlines have been installed as shown in Fig. 1. The 0.8 GeV compact linac in the undulator hall supplies electron beams to BL1. The 8-GeV SACLA main linac in the accelerator tunnel supplies electron beams to two XFEL beamlines, BL2 and BL3 in a pulse-by-pulse switching manner. A self-modulated energy chirp is mainly formed through the main C-band accelerator section between BC3 where the bunch is fully compressed and the exit of C-band accelerator. Additional bunch compression with the self-modulated energy chirp will be took place at the dog-leg section with R_{56} adjusted positive to generate attosecond XFEL at BL2. The BL3 chicane for the dark current suppression will be replaced by a compact R_{56}-positive magnetic chicane to generate attosecond XFEL at BL3. The design detail of a compact chicane with positive-R_{56} will be described below.

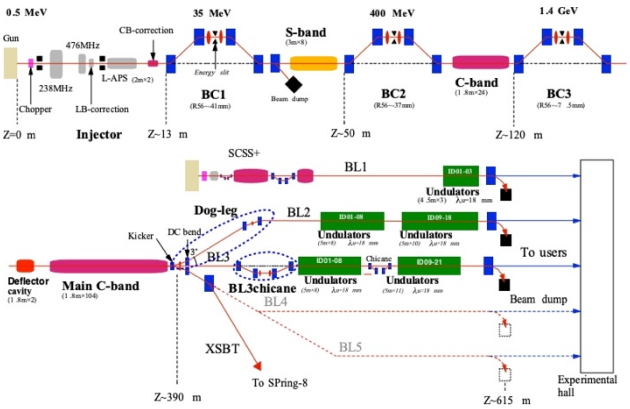

Figure 1: SACLA accelerator system.

CHICANE WITH POSITIVE R_{56}

To realize a magnetic chicane with positive R_{56}, the path length of an electron of lower energy than design ($\delta = \Delta p/p < 0$) must be shorter than that of higher energy ($\delta > 0$). This relationship between the energy and the path length is opposite to that of usual chicanes, and reversing this relationship can be achieved by installing focusing quadrupoles at dispersive sections so that the electron with $\delta > 0$ ($\delta < 0$) passing through the outer (inner) trajectory is kicked inward (outward). In Fig. 2 we show an example of such a chicane having a positive value of $R_{56} = +350$ μm. In this design, the length and the field of bending magnets are 0.35 m and 0.482 T at 8 GeV, respectively, and B2 and B3 have the opposite polarity of B1 and B4.

The value of R_{56} must be tunable within a certain range under the condition that the magnetic field of bending magnets is fixed. By adjusting the quadrupole fields inside the chicane, one can change the dispersion pattern as shown in Fig. 3. Figure 4 shows the quadrupole field strengths (left) and R_{56} (right) as a function of the peak value of the dispersion function $\eta^{(peak)}$. We expect that the necessary R_{56} for bunch compression in SACLA BL3 will be around a few hundred micrometers and the present tuning range seems to be wide enough for our purposes. The field

† email address: tanaka@spring8.or.jp

ISBN: 978-3-95450-248-6 ISSN: 2673-5490 doi: 10.18429/JACoW-IPAC2025-MOPB033

strength of quadrupoles in the chicane is slightly stronger than other sections. One of the reasons is that, as shown in Fig. 1, the space available for inserting a chicane in BL3 is limited between the route-switching kicker system and the first undulator, being about 40 m. It is then required to adopt a compact lattice design and the resulting field strength of quadrupoles becomes strong. The quadrupoles outside the chicane (see Fig. 2) are used for optics matching at each value of $\eta^{(peak)}$.

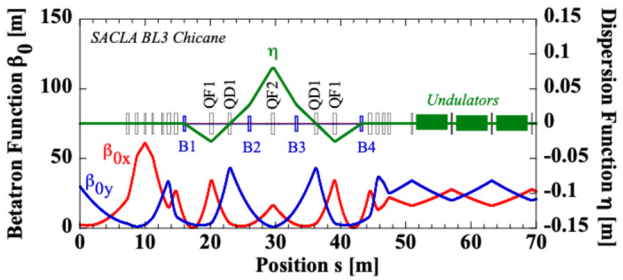

Figure 2: An example of a new BL3 chicane with positive R_{56}. The black and blue squares represent quadrupole and bending magnets, respectively.

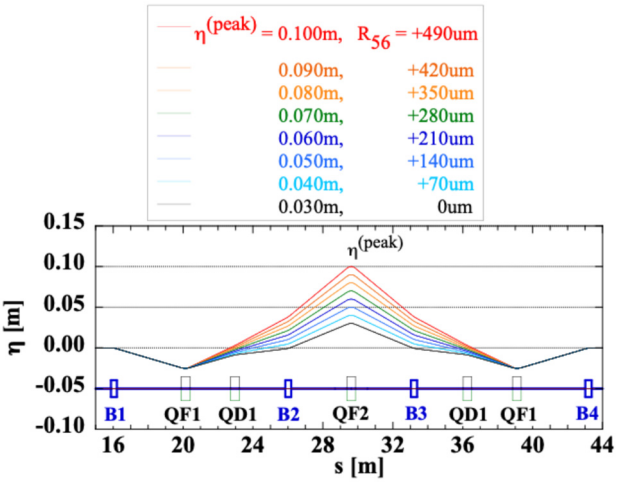

Figure 3: The dispersion function inside the chicane, whose peak value $\eta^{(peak)}$ can be changed by adjusting the strength of quadrupoles QF1, QD2 and QF2.

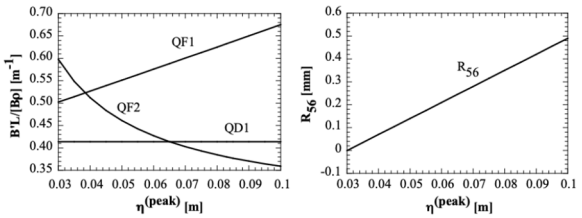

Figure 4: Tunability of R_{56}: quadrupole field strengths (left) and R_{56} (right) are shown as a function of $\eta^{(peak)}$.

CHROMATIC EFFECTS

Effects on Emittance

After designing the chicane lattice, we carried out computer simulations by using the code ELEGANT [7], and we found that when we insert a chicane with a positive R_{56} of a few hundred micrometers, the slice emittance is increased by about 50% in both horizontal and vertical directions. To understand the reason for this emittance increase, we further examined by checking the effects of synchrotron radiation, CSR, higher order dispersion, etc. and we finally concluded that the chromatic aberration cannot be neglected and it is the main reason that causes the emittance increase since the field of quadrupole magnets of the chicane is stronger than other sections as explained. The energy spread of the electron beam is not so small (up to about $\pm$0.5%) and after passing through the chicane the transverse phase space disperses. This emittance increase has a non-negligible effect on user experiments and must be compensated for. We discuss it in the next section.

Correction Scheme

We start by considering the energy (δ) dependence of the transfer matrix M_x of the chicane section [8]:

$$\begin{pmatrix} x^{(out)} \\ x'^{(out)} \end{pmatrix} = M_x \begin{pmatrix} x^{(in)} \\ x'^{(in)} \end{pmatrix}, \quad (1)$$

$$M_x = M_{0,x} + M_{1,x}\delta, \quad (2)$$

where we have explicitly separated the δ-dependent part as $M_{1,x}$. (In this paragraph we describe only the horizontal (x) direction, but the same applies to the vertical (y) direction.) The matrix M_x is obtained by concatenating that for each element $M_x^{(i)}$ (i=1,2,...,n) included in the lattice:

$$M_x = M_x^{(n)} M_x^{(n-1)} \dots M_x^{(2)} M_x^{(1)}. \quad (3)$$

By separating the δ-dependent part of each matrix $M_x^{(i)}$ as

$$M_x^{(i)} = M_{0,x}^{(i)} + M_{1,x}^{(i)}\delta, \quad (4)$$

we obtain

$$M_{0,x} = M_{0,x}^{(n)} M_{0,x}^{(n-1)} M_{0,x}^{(n-2)} \dots M_{0,x}^{(2)} M_{0,x}^{(1)}, \quad (5)$$

$$\begin{aligned} M_{1x} = {} & M_{1,x}^{(n)} M_{0,x}^{(n-1)} M_{0,x}^{(n-2)} \dots M_{0,x}^{(2)} M_{0,x}^{(1)} \\ & + M_{0,x}^{(n)} M_{1,x}^{(n-1)} M_{0,x}^{(n-2)} \dots M_{0,x}^{(2)} M_{0,x}^{(1)} \\ & + \dots + M_{0,x}^{(n)} M_{0,x}^{(n-1)} M_{0,x}^{(n-2)} \dots M_{0,x}^{(2)} M_{1,x}^{(1)}. \end{aligned} \quad (6)$$

The δ-independent part $M_{0,x}^{(i)}$ is well known, and the δ-dependent part $M_{1,x}^{(i)}$ for the quadrupole magnet is

$$M_{1,x}^{(QF)} = \begin{pmatrix} \frac{u}{2}\sin u & -\frac{L}{2}\cos u + \frac{L}{2u}\sin u \\ -\frac{u^2}{2L}\cos u + \frac{u}{2L}\sin u & \frac{u}{2}\sin u \end{pmatrix}, \quad (7)$$

$$M_{1,x}^{(QD)} = \begin{pmatrix} -\frac{u}{2}\sinh u & -\frac{L}{2}\cosh u + \frac{L}{2u}\sinh u \\ -\frac{u^2}{2L}\cosh u - \frac{u}{2L}\sinh u & -\frac{u}{2}\sinh u \end{pmatrix}, \quad (8)$$

where $u \equiv L\sqrt{|B'|/[B\rho]}$, L is the magnet length and $[B\rho]$ is the magnetic rigidity.

ISBN: 978-3-95450-248-6 ISSN: 2673-5490 doi: 10.18429/JACoW-IPAC2025-MOPB033

The basic idea of our correction scheme is that if

$$M_{1,x} = M_{1,y} = O, \tag{9}$$

the chromatic aberration cancels at the exit of the chicane. Though the aberration remains inside the chicane, the photon beam performance will not be affected by this.

A naive way to satisfy Eq. (9) will be to install an appropriate number of sextupole magnets at the dispersive section as independent tuning knobs. The expression of $M_{1,x}^{(i)}$ and $M_{1,y}^{(i)}$ for a thick sextupole magnet is given in [8] (see Eqs. (37) and (38)), but for our present purpose the thin lens approximation will be enough:

$$M_{1,x}^{(SX)} = \begin{pmatrix} 0 & 0 \\ -K_1 L\eta^{(SX)} & 0 \end{pmatrix}, \tag{10}$$

$$M_{1,y}^{(SX)} = \begin{pmatrix} 0 & 0 \\ +K_1 L\eta^{(SX)} & 0 \end{pmatrix}, \tag{11}$$

where $K_1 \equiv B''/[B\rho]$ is the strength of the sextupole magnet and $\eta^{(SX)}$ is the dispersion function at this position. Equation (9) is a 2×2 matrix equation and we have eight relations in total. However, from the relation $detM_x = detM_y = 1$, the following constraints are always satisfied:

$$Tr\left[M_{0,x}^{-1}M_{1,x}\right] = Tr\left[M_{0,y}^{-1}M_{1,y}\right] = O, \tag{12}$$

This reduces the number of independent equations by two and Eq. (9) can be satisfied by six independent variables.

From Eqs. (6) and (9) we have

$$\sum_{i\in SEXTUPOLE} M_{0,x}^{(n)}M_{0,x}^{(n-1)}\dots M_{0,x}^{(i+1)}M_{1,x}^{(i)}M_{0,x}^{(i-1)}\dots M_{0,x}^{(1)} =$$

$$-\sum_{i\in QUAD} M_{0,x}^{(n)}M_{0,x}^{(n-1)}\dots M_{0,x}^{(i+1)}M_{1,x}^{(i)}M_{0,x}^{(i-1)}\dots M_{0,x}^{(1)}, \tag{13}$$

and a similar expression for the vertical direction. The sextupole strengths appear only on the left-hand side through $M_{1,x}^{(i)}$ (and $M_{1,y}^{(i)}$) and Eq. (13) can be reduced to the linear matrix equation of the form

$$AX = B, \tag{14}$$

where X is a column vector representing a set of sextupole strengths. Equation (14) can be solved using, for example, SVD.

The Twiss parameters (β, α, γ) are transferred by the following equation (Eq. (24) of [8]):

$$\sigma^{(out)} = M\sigma^{(in)}M^T, \tag{15}$$

where

$$\sigma = \begin{pmatrix} \beta & -\alpha \\ -\alpha & \gamma \end{pmatrix}. \tag{16}$$

By separating the δ-dependent part as

$$\sigma = \sigma_0 + \sigma_1\delta. \tag{17}$$

where

$$\sigma_0 = \begin{pmatrix} \beta_0 & -\alpha_0 \\ -\alpha_0 & \gamma_0 \end{pmatrix}, \quad \sigma_1 = \begin{pmatrix} \beta_1 & -\alpha_1 \\ -\alpha_1 & \gamma_1 \end{pmatrix}, \tag{18}$$

$$\beta = \beta_0 + \beta_1\delta, \quad \alpha = \alpha_0 + \alpha_1\delta, \quad \gamma = \gamma_0 + \gamma_1\delta, \tag{19}$$

and using Eq. (2), we have

$$\sigma_1^{(out)} = M_0\sigma_1^{(in)}M_0^T + M_1\sigma_0^{(in)}M_0^T + M_0\sigma_0^{(in)}M_1^T. \tag{20}$$

At the entrance of the chicane, the δ-dependent term of the Twiss parameters is expected to be small and we may put $\sigma_1^{(in)} \cong 0$. Then, Eq. (20) is reduced to

$$\sigma_1^{(out)} \cong M_1\sigma_0^{(in)}M_0^T + M_0\sigma_0^{(in)}M_1^T. \tag{21}$$

When Eq. (9) is satisfied, the right-hand side of Eq. (21) becomes always zero and the energy dependence of the Twiss parameters disappears at the exit of the chicane *regardless of the initial values at the entrance* $\sigma_0^{(in)}$. This is very desirable for the linac since, unlike the storage ring, the Twiss parameters at the entrance cannot be determined without ambiguity and sometimes fluctuate shot-by-shot. Satisfying Eq. (9), even in an approximate way, is an important requirement from a practical point of view.

We distributed sextupole magnets in the model chicane shown in Fig. 2 and solved Eq. (14) using SVD. This is equivalent to satisfying Eq. (9). We then tried to optimize sextupole strengths by changing the singular value threshold and sextupole positions. The resulting strengths were however too strong being about 50-150 m^{-2} and cannot be accepted. The reason why correction sextupoles become so strong will be that in designing the chicane as shown in Fig. 2, we have not considered the off-energy conditions Eq. (9). If these conditions were taken into account from the beginning, a better solution could be found. We are now trying to optimize the lattice by adding quadrupole magnets as tuning knobs to relax the required sextupole strengths.

SUMMARY

We have presented a novel design of a compact magnetic chicane with positive R_{56} for attosecond XFEL generation in SACLA BL3. This chicane has a wide enough tunability for covering the necessary R_{56} for bunch compression. Due to the compactness of the chicane, however, the strength of quadrupole magnets tends to be strong compared to other sections and this causes a non-negligible chromatic effect on the emittance. We then presented a correction scheme to compensate for this effect. Studies are ongoing to realize a compact and chromatic aberration-free chicane with positive R_{56} for attosecond XFEL generation.

ISBN: 978-3-95450-248-6 ISSN: 2673-5490 doi: 10.18429/JACoW-IPAC2025-MOPB033

REFERENCES

[1] J. Yan *et al.,* "Terawatt-attosecond hard X-ray free-electron laser at high repetition rate", *Nat. Photonics*, vol. 18, no. 12, pp. 1293–1298, Nov. 2024. doi:10.1038/s41566-024-01566-0

[2] T. Ishikawa *et al*., "A compact X-ray free-electron laser emitting in the sub-ångström region", *Nat. Photonics*, vol. 6, no. 8, pp. 540–544, Jun. 2012. doi:10.1038/nphoton.2012.141

[3] K. Togawa *et al.*, "CeB6 electron gun for low emittance injector", *Phys. Rev. Spec. Top. Accel. Beams*, vol. 10, No. 2, p. 020703, Feb. 2007. doi:10.1103/PhysRevSTAB.10.020703

[4] T. Inagaki *et al.*, "High-gradient C-band linac for a compact x-ray free-electron laser facility", *Phys. Rev. Spec. Top. Accel. Beams*, vol. 17, no 8, p. 080702, Aug. 2014. doi:10.1103/PhysRevSTAB.17.080702

[5] H. Kitamura, "Recent trends of insertion-device technology for X-ray sources", *J. Synchrotron Rad*., vol. 7, no.3, pp. 121-130, May 2000. doi:10.1107/S0909049500002983

[6] H. Maesaka, T. Hara, K. Togawa, T. Inagaki, and H. Tanaka, "Brightness analysis of an electron beam with a complex profile", *Phys. Rev. Accel. Beams*, vol. 21, no. 5, May 2018. doi:10.1103/physrevaccelbeams.21.050703

[7] M. Borland, "ELEGANT: A Flexible SDDS-Compliant Code for Accelerator Simulation", Technical Report LS-287, APS, 2000.

[8] B. Autin and A. Verdier, "Focusing Perturbations in Alternating Gradient Structures", CERN, Geneva, Switzerland, CERN ISR-LTD/76-14, 1976.